Available online at www.sciencedirect.com
ScienceDirect
Chinese Journal of Natural Medicines 2020, **18**(5): 345–355
doi: 10.1016/S1875-5364(20)30041-8
Chinese Journal of Natural Medicines

•Research article•

Cordycepin inhibits pancreatic cancer cell growth *in vitro* and *in vivo* via targeting FGFR2 and blocking ERK signaling

LI Xue-Ying[1, 2Δ], TAO Hong[1Δ], JIN Can[1Δ], DU Zhen-Yun[1], LIAO Wen-Feng[1], TANG Qing-Jiu[3*], DING Kan[1*]

[1] *Glycochemistry & Glycobiology Lab, Key Laboratory of Receptor Research, Shanghai Institute of Materia Medica, Chinese Academy of Sciences, Shanghai 201203, University of Chinese Academy of Sciences, Beijing 100049, China;*
[2] *College of Pharmacy, Nanchang University, Nanchang 330006, China;*
[3] *Institute of Edible Fungi, Shanghai Academy of Agricultural Science, Shanghai 201203, China*

Available online 20 May, 2020

[ABSTRACT] Cordycepin (3′-deoxyadenosine) from *Cordyceps militaris* has been reported to have anti-tumor effects. However, the molecular target and mechanism underlying cordycepin impeding pancreatic cancer cell growth *in vitro* and *in vivo* remain vague. In this study, we reported functional target molecule of cordycepin which inhibited pancreatic cancer cells growth *in vitro* and *in vivo*. Cordycepin was confirmed to induce apoptosis by activating caspase-3, caspase-9 and cytochrome c. Further studies suggested that MAPK pathway was blocked by cordycepin via inhibiting the expression of Ras and the phosphorylation of Erk. Moreover, cordycepin caused S-phase arrest and DNA damage associated with activating Chk2 (checkpoint kinase 2) pathway and downregulating cyclin A2 and CDK2 phosphorylation. Very interestingly, we showed that cordycepin could bind to FGFR2 ($K_D = 7.77 \times 10^{-9}$) very potently to inhibit pancreatic cancer cells growth by blocking Ras/ErK pathway. These results suggest that cordycepin could potentially be a leading compound which targeted FGFR2 to inhibit pancreatic cells growth by inducing cell apoptosis and causing cell cycle arrest via blocking FGFR/Ras/ERK signaling for anti-pancreatic cancer new drug development.

[KEY WORDS] Cordycepin; FGFR2; Apoptosis; Pancreatic cancer; Ras/Erk
[CLC Number] R965 **[Document code]** A **[Article ID]** 2095-6975(2020)05-0345-11

Introduction

Pancreatic ductal adenocarcinoma (PDAC) is one of the most fatal cancers, owing to its poor clinical diagnosis and chemoresistance [1]. Moreover, the tumor is often inoperable at diagnosis due to its severe metastasis and invasiveness [2]. Gemcitibine has been recommended as the standard first-line treatment for pancreatic cancer since 1997 [3], whereas offering weak efficacies but strong resistance [4]. Therefore, novel therapeutic treatments are urgently needed.

Fibroblast growth factors (FGFs) consist of 22 different growth factors that regulate embryonal development, wound healing, cell proliferation and survival by binding to fibroblast growth factor receptors (FGFR) and activating downstream pathways [5-8]. Aberrant FGF signaling has a unique and critical role in the development of malignant tumor. It is reported that FGF signaling pathway shows the highest enrichment containing non-synonymous mutations for different kinase genes [9]. Clinical histopathology studies have shown that the increasing production of bFGF secreted by pancreatic cancer cells induces further hyperplastic lesions of the pancreas [10]. Moreover, FGFR2, the subtype 2 receptor for FGF, is overexpressed in pancreatic tumor. Hence, targeting FGFR2 and regulating its downstream pathways might be a therapeutic strategy in PDAC. FGF-stimulation on FGFR results in activation of the Ras/Mitogen-activated protein kinase (MAPK) signaling cascade [11]. There is evidence that overactivated ERK MAPK signaling pathway is responsible for human oncogenesis and is involved in aberrant development in cancers [12]. In addition, the ERK MAPK signaling plays an important role in regulating cell growth, apoptosis, cell cycle arrest and so on [13].

[Received on] 18-Oct.-2019
[Research funding] This work was supported by Strategic Priority Research Program of the Chinese Academy of Sciences (No. XDA12010302) and National Natural Science Foundation of China (No. 31230022) and Program of Shanghai Subject Chief Scientist (No. 16XD1404500).
[*Corresponding author] Tel: 86-21-62205130, E-mail: tangqingjiu@saas.sh.cn; (TANG Qing-Jiu); Tel: 86-21-50806928, Fax: 86-21-50806928, E-mail: dingkan@simm.ac.cn (DING Kan)
[Δ]These authors contributed equally to this work.
These authors have no conflict of interest to declare.

Cordycepin (3′-deoxyadenosine), a naturally nucleoside analog, is the major bioactive component isolated from *Cordyceps militaris*. More evidences have shown that cordycepin may inhibit tumor cells growth [14-18]. Recently, Zhang *et al.* reported that cordycepin might induce human pancreatic cancer cells apoptosis and suppress the tumor growth *in vivo* [17]. However, its functional molecular target and the related mechanism of action remain unclear. In this study, we show evidence that cordycepin inhibits pancreatic cancer cells growth *in vitro* and *in vivo* by targeting FGFR2 and blocking ERK/MAPK signaling.

Material and Method

Reagents

Cordycepin was prepared in Institute of Edible Fungi, Shanghai Academy of Agricultural Sciences and extracted from *Cordyceps militaris* by macroporous resin [19]. 3-(4, 5-dimethylthiazol-2-yl)-2, 5-diphenyl tetrazolium bromide (MTT) was from sigma-Aldrich, USA. Dimethyl Sulfoxide (DMSO) was purchased from E. Merck, Germany. aFGF and FGFR2 were purchased from Sino Biological (Beijing, China). aFGF (Sino Biological, Cat #: 10013-HNAE; Sources from Human, A DNA sequence encoding the mature form of human FGF acidic (AAA79245.1) (Phe 16-Asp 155) was expressed, with an additional Met at the N-terminus. E. Coli expressed, activity measured in a cell proliferation assay using BALB/c 3T3 mouse fibroblasts. The ED50 for this effect is typically 50–200 pg·mL^{-1}). FGFR2 (Sino Biological, Cat #: 10824-H08H; Sources from Human, A DNA sequence encoding the human FGFR2 (NP_000132.3) extracellular domain (Met 1-Glu 377) was expressed, fused with a polyhistidine tag at the C-terminus. HEK293 Cells expressed, Measured by its ability to inhibit FGF acidic dependent proliferation of Balb/c3T3 mouse embryonic fibroblasts. The ED50 for this effect is typically 200–400 ng·mL^{-1}). Other reagents were obtained from Sinopharm Chemical Reagent Co., Ltd. (Shanghai, China).

Cells culture

All cells were obtained from the Cell Bank in the Type Culture Collection Center of the Chinese Academy of Sciences, Shanghai, China. The pancreatic cancer cell line BxPC-3 and AsPC-1, and the normal pancreatic cell line HPDE6-C7 were maintained in RPMI-1640 medium containing 10%FBS and antibiotics (100 U·mL^{-1} penicillin, 100 μg·mL^{-1} streptomycin, Invitrogen). The pancreatic cancer cell line PANC-1 was cultured in DMEM medium supplemented with 10% FBS and antibiotics (100 U·mL^{-1} penicillin, 100 μg·mL^{-1} streptomycin, Invitrogen). These cell lines were all cultured at 37 °C in a 5% CO_2 incubator.

MTT assay

BXPC-3 (3×10^3 cells/well) cells were seeded into 96-well plate and incubated under normal culture condition overnight. Then cells were cultured with or without cordycepin for 72 h, and incubated with 5 mg·mL^{-1} of MTT (3-[4, 5-dimethyl thiazol-2-yl]-2,5-diphenyl tetrazolium bromide) for another 4 h. The formazan crystals produced from MTT in the living cells were dissolved in dimethyl sulfoxide (DMSO). The color absorbance was detected at 490 nm by a spectrophotometer (Thermo Scientific, West Palm Beach, FL). The effect of cordycepin on cell viability was calculated as (sample/control) × 100%.

Western blotting

Total protein was extracted by lysing cells with an equal volume of the RIPA buffer (Beyotime, China). The cytoplasmic protein was isolated using Nuclear and Cytoplasmic Protein Extraction Kit (Sangon Biotech, China). The protein samples were separated by SDS–polyacrylamide gel electrophoresis and transferred onto a polyvinyl difluoride (PVDF) membrane (Life Science). After blocking with 5% nonfat milk for 2 h, the membrane was incubated with primary antibodies overnight at 4 °C, followed by incubation with secondary antibodies for 2 h, the blots were visualized with enhanced chemilumine-scene reagent (Pierce). Antibodies used were listed in Supplementary Table S1.

Colony formation

BxPC-3 cells (1×10^3 cells/well) were seeded and incubated in a 6-well plate overnight and then treated with different concentrations of cordycepin. The medium containing cordycepin was replaced every 3 days. After 2 weeks, the colonies were clearly visible and stained with Giemsa for counting.

RNA extraction, RT–PCR and quantitative real-time PCR

After cordycepin treatment, total RNA was extracted from cultured cells using Trizol reagent (Invitrogen, USA). Complementary DNA (cDNA) was synthesized from 2 μg total RNAs using M-MLV reverse transcriptase (Takara Biotechnology, Dalian, China). Then PCR amplification was performed with rTaq (Takara Biotechnology, China) following the manufacturer's instructions. PCR primers were shown in Supplementary Table S1.

Surface plasmon resonance (SPR) analysis

SPR measurements for binding affinity analysis were conducted on a BIACORE T200 (GE Healthcare, Stockholm, Sweden). The human recombinant proteins were immobilized to a CM5 sensor chip by a standard amine coupling method. Different concentrations of cordycepin or aFGF dissolved in HBS-EP buffer (150 mol·L^{-1} NaCl, 3 mmol·L^{-1} EDTA, 10 mol·L^{-1} HEPES and 0.05% surfactant P20, pH 7.4) were injected onto the sensor chips. In competitive inhibition assays, certain concentration of aFGF (29.67 nmol·L^{-1}) was incubated with increasing concentrations of cordycepin and then injected to the chip. Kinetic parameters were evaluated by BIACORE T200 Evaluation Software Version 1.0.

Transwell assay

Transwell assay was used to evaluate migration ability. BxPC-3 cells (1×10^5 cells/well) in 100 μL of serum-free medium were seeded in the upper chamber. And the lower chamber was filled with medium containing 10% FBS and different concentrations of cordycepin. After 8 h incubation, the migrated cells were stained by 0.1% crystal violet and then photographed by a microscope (Olympus BX51).

Apoptosis and cell cycle analysis by flow cytometry

Cells (3×10^5 cells/well) were seeded in a 6-well plate and incubated overnight. After treatment, cells were harvested using 0.25% Tyrisin and washed with cold PBS. Cells were fixed in ice-cold 75% ethanol at 4 °C overnight. After washing, the cells were incubated with PBS containing RNase A (100 μg·mL^{-1}) in 37 °C water bath for 1 h and incubated on the ice with 50 μg·mL^{-1} PI (Invitrogen, USA) for 15 mins, the DNA content was measured by flow cytometry with Modfit LT 3.0 software (Becton Dickinson, Franklin Lakes, NJ). Apoptotic or necrotic cells were stained with Alexa®Flour 488 Annexin V and PI, afterwards the samples were analyzed on FACSCalibur (Becton Dickinson).

Xenograft model

All animal studies were carried out according to the Guide for the Care and Use of Laboratory Animals of the National Institutes of Health. BxPC-3 cells (3×10^6 cells/mouse) were subcutaneously injected into the flank of female BALB/cA nu/nu mice (6–8 weeks old). Xenografted animals were treated daily with cordycepin (10 mg·kg^{-1}) in saline via oral administration, and animals from control group were treated with equivalent volumes of normal saline when tumor was palpable. The tumor volume (V) was calculated as followed: $V = (\text{length} \times \text{width}^2)/2$. On the 32nd day, mice were euthanized and tumor tissues were excised.

Immunohistochemistry

Tumors were excised and fixed in 4% paraformaldehyde, then embedded in paraffin and sectioned for immunohistochemical analysis. Cell proliferation was evaluated by staining the sections with Ki67 antibody (CST). The expression of ERK phosphorylation was showed by staining p-Erk antibody (CST). Semiquantitative image analysis was used by Image Pro Plus software.

Statistical analysis

All data were presented as mean values ± SEM. P-value of the difference between groups were analyzed with Student's t-test, a single factor analysis of variance and unpaired using the PRISM software (GraphPad Software). Values of P less than 0.05 were considered statistically significant. ($^{*}P < 0.05$, $^{**}P < 0.01$, $^{***}P < 0.001$).

Results

Cordycepin (3′-deoxyadenosine) inhibited PDAC cells in vitro and in vivo

MTT assay was used to test the effect of cordycepin on pancreatic cancer cell viability. As shown in Fig. 1A, cordycepin inhibited the cell viabilities of pancreatic cancer cells BxPC-3, CFPAC-1, AsPC-1, PANC-1 and SW1990 in a dose-dependent manner. IC_{50} of cordycepin on these five cell lines were 38.85, 72.99, 150.1, 213.1, 349.3 μmol·L^{-1}, respectively. Obviously, BxPC-3 cells were more sensitive to cordycepin treatment. The inhibition rate of this compound on BxPC-3 cells at the concentration of 100 μmol·L^{-1} was around 90%. However, cordycepin nearly had no toxicity on normal pancreatic cell line HPDE6-C7 at its effective concentration (Fig. 1B). These results indicated that cordycepin might have negligible toxic effects on normal pancreatic tissues at least under the effective dose.

Furthermore, we detected the effects of cordycepin on the colony formation and migration of BxPC-3 cells. As shown in Fig. 1C and Fig. 1D, cordycpein significantly reduced the size of BxPC-3 colonies and inhibited migration of BxPC-3 cells at the concentration of 50 or 100 μmol·L^{-1}.

To determine whether cordycepin could inhibit tumor growth *in vivo*, tumor xenograft model was employed in this study. Tumor volume was calculated every 3 or 4 days for 32-day treatment. The results showed that cordycepin significantly reduced BxPC-3 xenograft tumor growth and tumor weights (Figs. 1E–1G). Moreover, the body weights of mice showed no significant changes comparing to the control group (Fig. 1H). The above results suggest that cordycpein could inhibit the tumor growth without significant side effects.

Cordycepin induced apoptosis in BxPC-3 cells

Inducing apoptosis of tumor cells is general strategy of anti-tumor agents. After treated with 50 and 100 μmol·L^{-1} cordycepin for 48 h, the percentage of apoptotic cells of control, 50 and 100 μmol·L^{-1} groups was 3.68%, 29.48%, and 43.79%, respectively ($P < 0.001$, Fig. 2A). To understand the underlying mechanism, the activation of caspase-3 and caspase-9, which played significant roles in cell apoptosis were analyzed [20]. Western blotting results indicated that the expressions of cleaved caspase-3 and caspase-9 were significantly upregulated by cordycepin treatment (Fig. 2B). Caspase 9 could be triggered by the release of cytochrome c [21]. Therefore, we detected cytochrome c as well. Indeed, the release of cytochrome c into the cytosol was increased after cordycepin treatment (Fig. 2C). Bax, one of the members of BCL-2 family, is known to trigger apoptosis [22]. As expected, Bax and FasL were dramatically upregulated in cordycepin treated group (Fig. 2D). These data demonstrated that caspases pathway might be critical for cordycepin-induced BxPC-3 cells apoptosis.

Cordycepin induced BxPC-3 cells cycle arrest

To further explore the cell growth inhibition of cordycepin, BxPC-3 cells treated with 100 μg·L^{-1} cordycepin were analyzed by flow cytometry after propidium iodide (PI) staining. The percentage of cells in S phase was increased dose-dependently, indicating that cordycepin arrested BxPC-3 cells in S phase (Figs. 3A, 3B). Cyclin A2-CDK2 complex played an important role in regulating cell progression from G1 to S phase [23]. Cyclin A2 and CDK2 phosphorylationwere dramatically downregulated in the treatment group (Figs. 3C, 3E). Cyclin A2-CDK2 complex could be negatively regulated by p21 which belongs to Cip/Kip family [24]. Both of the mRNA level and protein level of p21 were increased in response to cordycepin treatment (Fig. 3D). In addition, the results showed that the phosphorylation of ATM, ATR and chk2 was upregulated (Fig. 3F), suggesting that cordycepin induced DNA damage. These results clearly illustrated that cordycpein induced S phase arrest via effecting the expres-

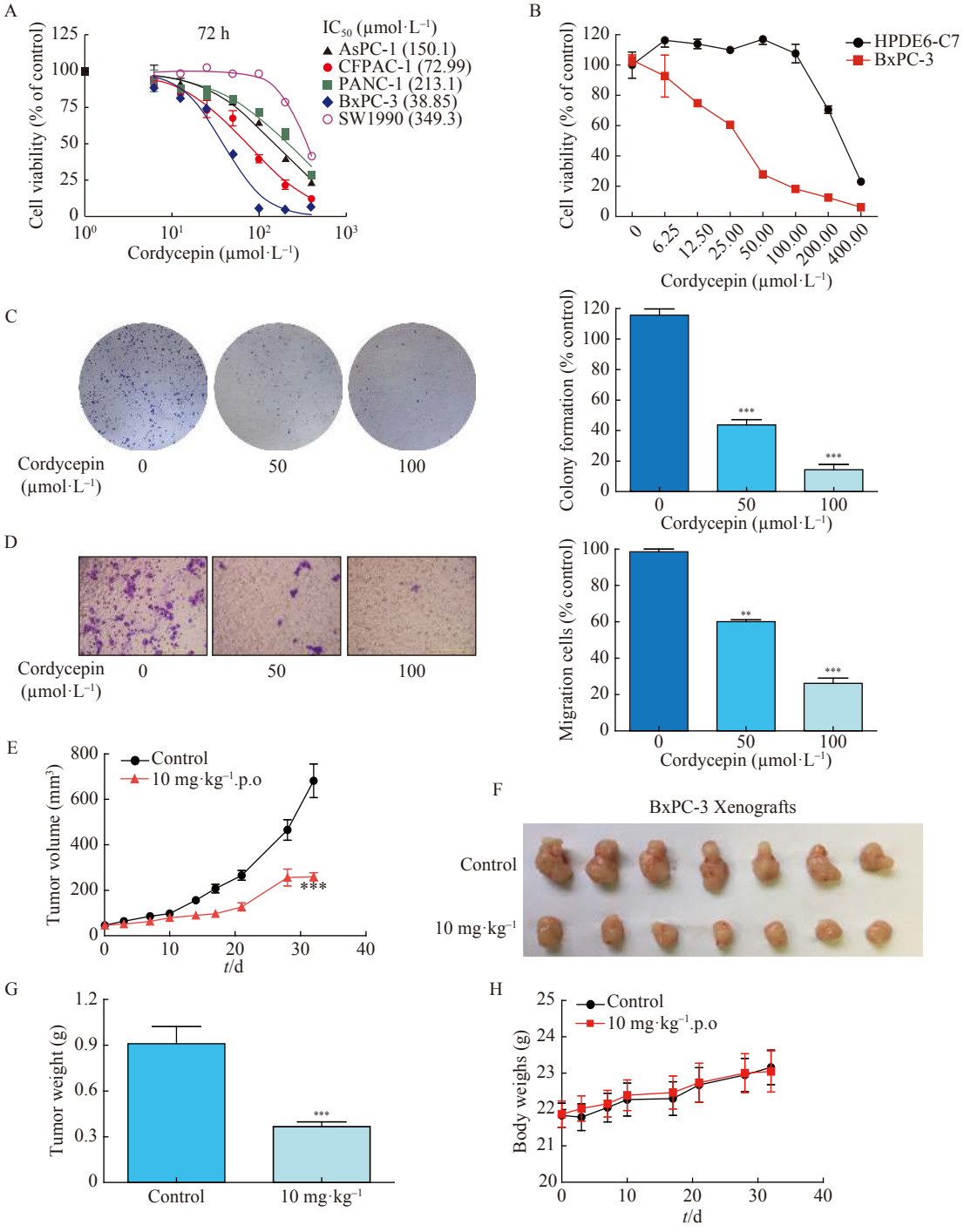

Fig. 1 Cordycepin (3′-deoxyadenosine) inhibited PDAC cells BxPC-3 *in vitro* and *in vivo*. (A) The cells were cultured with cordycepin (0, 6.25, 12.5, 25, 50, 100, 200, 400 μmol·L^{-1}) for 72 h. Cell viability was assessed by MTT assay. (B) The IC_{50} of cordycepin on BxPC-3 cells is 82.01 μmol·L^{-1} according to MTT assay. (C) Representative images of BxPC-3 colonies were shown after cordecepin treatment. BxPC-3 cells were incubated with cordycepin (0, 50, 100 μmol·L^{-1}) for 2 weeks. The colony size and the colony numbers were quantified for statistical analysis. The right panel showed the statistical analysis of colony formation. (D) BxPC-3 cells were treated with cordycepin (0, 50, 100 μmol·L^{-1}) for 8 h. The migration abilities were evaluated by Transwell assay and the migration cells were photographed. The right panel shows the statistical analysis of migration. (E) The curves of tumor volumes (mean ± SEM) indicate the tumor growth of cordycepin treatment group and control group. (F) The BxPc-3 xenograft tumors were photographed. (G) Excised tumor weights were measured. (H) The body weights of the nude mice were measured during the study. The experiments were repeated thrice. Data were represented as mean ± SEM; $^{**}P < 0.01$, $^{***}P < 0.001$

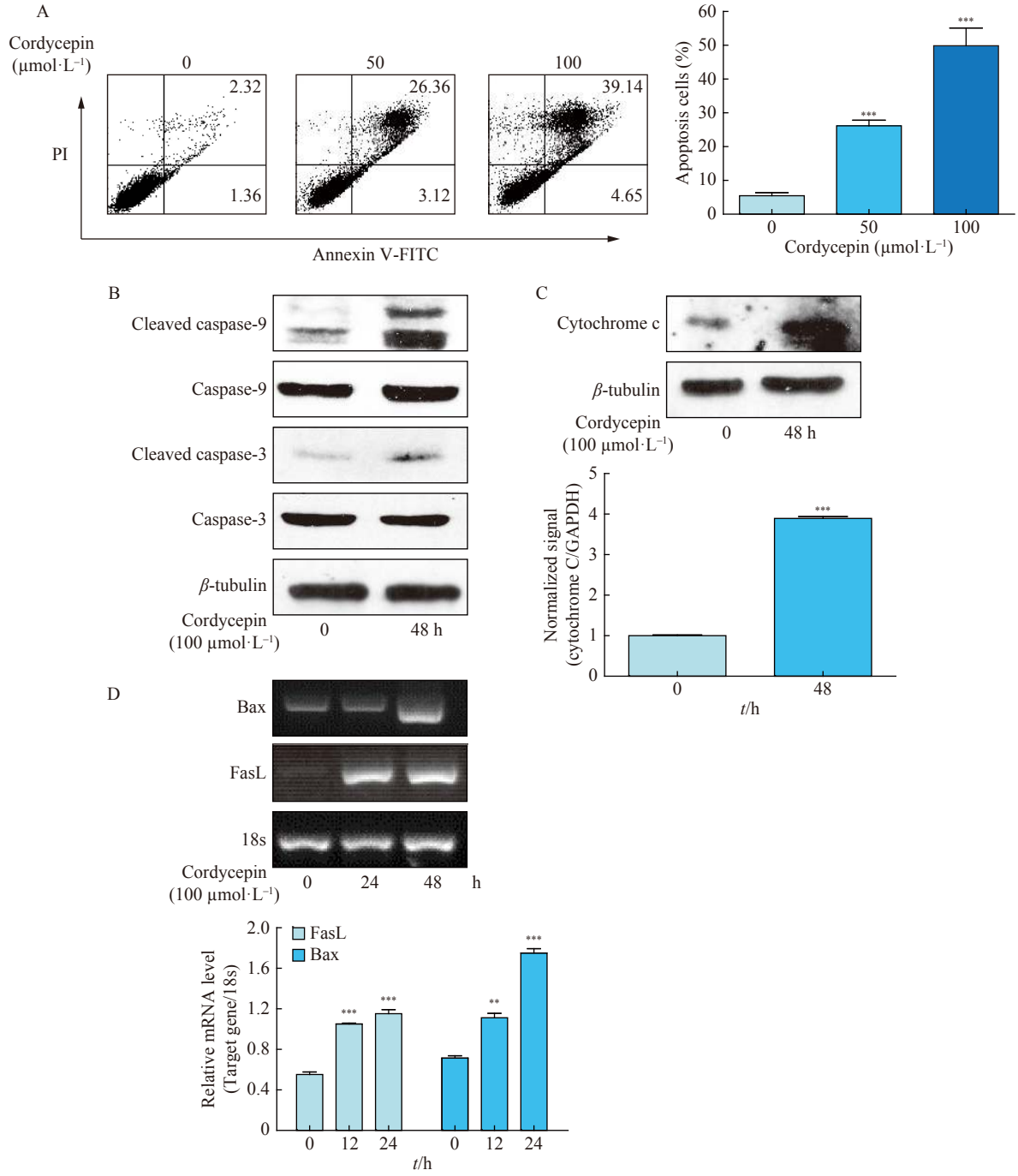

Fig. 2 Cordycepin induced apoptosis in BxPC-3 cells. (A) BxPC-3 cells were incubated with cordycepin (0, 50, 100 μmol·L^{-1}) for 48 h and stained with Annexin V and PI. Annexin V was analyzed by flow cytometry. (B and C) BxPC-3 cells were incubated with 100 μM cordycepin for indicated time. The protein levels of cleaved caspase-3, cleaved caspase-9 and Cytochrome c were measured by Western blotting. *β*-tubilin was used as a control for protein loading. (D) BxPC-3 cells were treated with 100 μmol·L^{-1} for indicated time. RT-PCR was employed to analyze mRNA level of Bax and FasL. Integrated optical densities of bands normalized by 18s were shown below. The experiments were repeated thrice. Data were represented mean ± SEM; $^{**}P < 0.01$; $^{***}P < 0.001$

sion and activation of cell cycle related proteins.

Cordycepin bound to FGFR2 and impaired aFGF-induced BxPC-3 cells growth

Fibroblast growth factors (FGFs) and Fibroblast growth factor receptor (FGFR) were implicated in tumor angiogenesis and their expression is high in clinical pancreatic tumor specimens [10]. We therefore sought to investigate whether cordycepin could disrupt FGF-induced cell growth. BxPC-3 cells were treated with aFGF (20 ng·mL^{-1}) or bFGF (20 ng·mL^{-1}), respectively. As expected, aFGF and bFGF significantly stimulated cell growth. Nevertheless, the effects were abrogated in the presence of cordycepin (100 μmol·L^{-1})

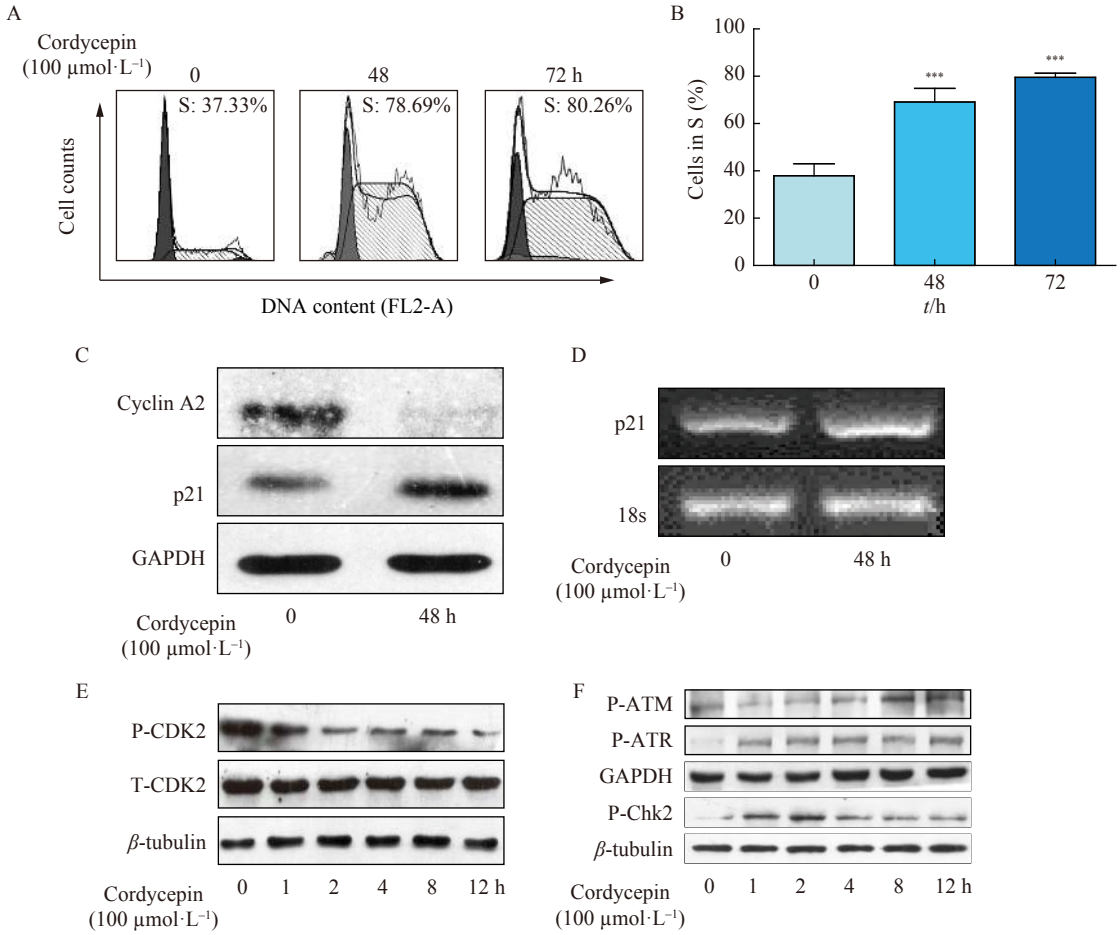

Fig. 3 Cordycepin induced BxPC-3 cells cycle arrest. (A and B) Cell cycle distribution of BxPC-3 cells were analyzed by flow cytometry after 100 μmol·L^{-1} cordycepin treatment for 48 h and 72 h. (C and D) BxPC-3 cells were incubated with 100 μmol·L^{-1} cordycepin for 48 h followed by expression measurement of cyclin A2, p21, GAPDH, 18S at protein and mRNA levels by Western blotting and PCR. (E and F) BxPC-3 cells were treated with cordycepin for indicated time. The phosphorylation of CDK2, ATM, ATR and Chk2 was measured by Western blotting. The experiments were repeated thrice. Data were represented as mean ± SEM; $^{***}P < 0.001$

(Fig. 4A, 4B), and the inhibition was more significant in aFGF treatment group. Results above showed that cordycepin could significantly inhibit aFGF induced cell growth, thus the role of aFGF involved was further investigated in this study.

The extracellular domain of FGFR consists of the acidic box, which was essential for interacting with heparin sulfate proteoglycan (HSPG) [25]. Cordycepin also contains free alkaline amino groups. Therefore we wonder whether cordycepin could interact with FGFR or/and aFGF as well. Firstly, Surface Plasmon Resonance (SPR) was employed to evaluate the affinity of aFGF to FGFR2, and the K_D value for aFGF-FGFR2 was 6.44×10^{-9} (Fig. 4C). Then we analyze the interaction of aFGF or FGFR2 in the presence of cordycepin (Fig. 4D). The results showed that there is almost no combination between aFGF and cordycepin (Fig. S2), whereas, the K_D value for FGFR2-cordycepin was 7.77×10^{-9}, suggesting similar affinity of ligand (aFGF) with receptor (FGFR2). We supposed whether the interaction of cordycepin with FGFR2 led to the inhibition of FGFR2 phosphorylation. The result showed that cordycepin suppressed the phosphorylation of FGFR2 (Fig. 4E). In addition, we also found that FGFR2 inhibitor AZD4574 could impede the cell viability of BxPC-3 cells (Figs. 4F, 4G). The observation above supports the hypothesis that aFGF plays a key role in cordycepin-driven cell growth inhibitory effects.

Cordycepin caused cell death via inhibiting ERK pathway

To confirm the molecular mechanism of cordycepin-induced cell death, we examined the effect on ERK signaling pathway, one of the downstream pathways of FGFR2. Treatment of BxPC-3 cells with 100 μmol·L^{-1} cordycepin for 12 or 24 h significantly decreased the phosphorylation of ERK and the expression of Ras ($P < 0.05$; Fig. 5A). In addition, the transcription factors (c-Fos, c-myc, stat1) implicated in ERK signaling were downregulated after cordycepin treated (Fig. 5B). When FGFR2 was inhibited by its inhibitor, AZD 4547, the ERK phosphorylation was decreased (Fig. 5C). We used the MEK inhibitor PD98059 which can inhibit ERK phosphorylation to treat BxPC-3 cells (Fig. 5D). After PD98059 (50 or 100 μmol·L^{-1}) treatment, the growth and mi-

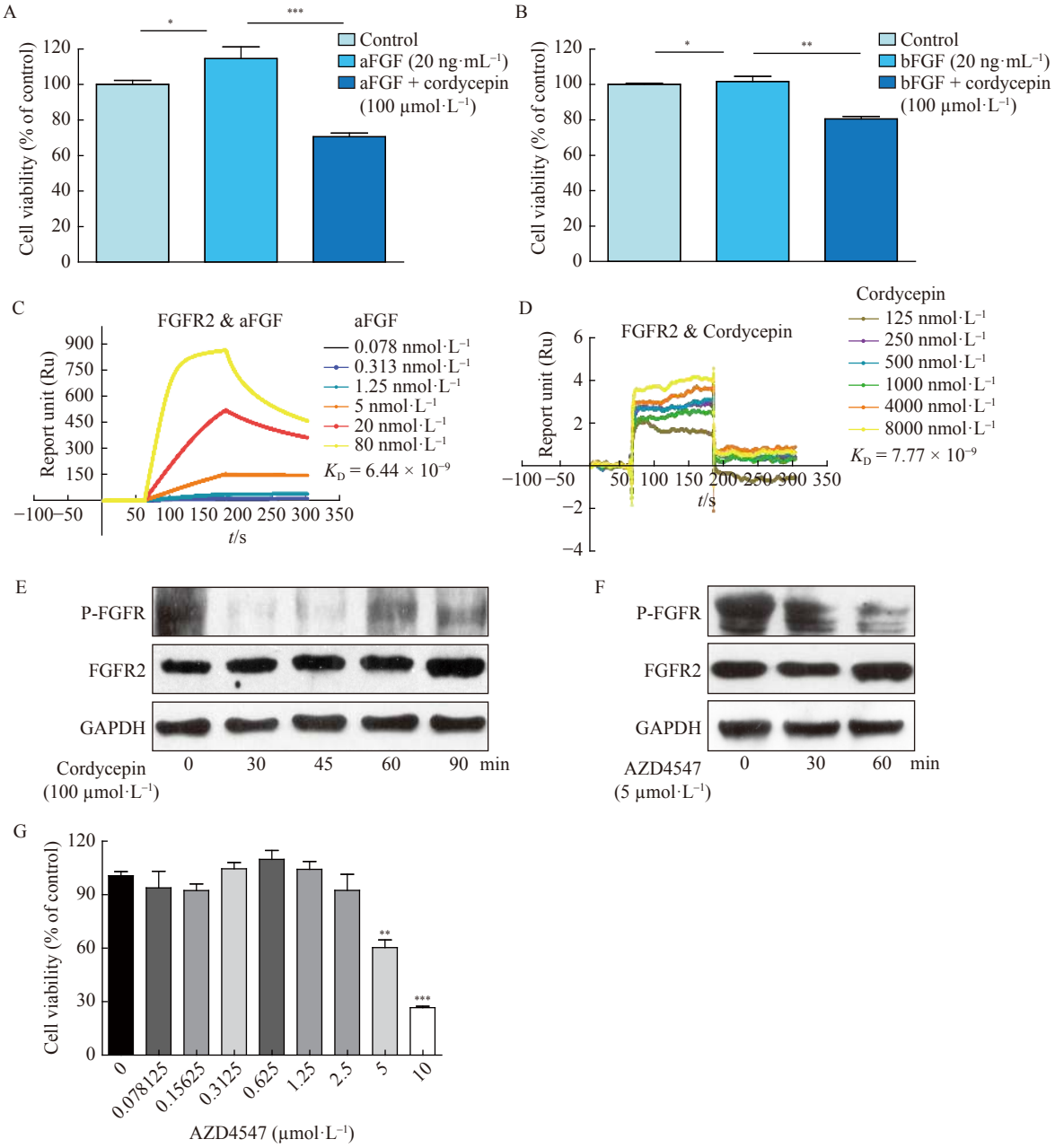

Fig. 4 Cordycpein bound to FGFR2 and impaired aFGF-induced BxPC-3 cells growth. (A and B) BxPC-3 cells were incubated with or without aFGF (20 ng·mL^{-1}) or bFGF (20 ng·mL^{-1}) and 100 μmol·L^{-1} cordycepin for 48 h. Cells viability was examined by MTT assay. (C and D) The interaction of different amounts of aFGF (C) or different amounts of cordycepin (D) in running buffer with immobilized FGFR2 obtained from Surface Plasmon Resonance analysis. (E) Phosphorylation of FGFR2 was examined by Western blotting after cordycepin treatment. (F) Phosphorylation of FGFR was analyzed by Western blotting after treated with 5 μmol·L^{-1} FGFR2 inhibitor (AZD4547) for 12 and 24 h. (G) BxPC-3 cells were incubated with different concentrations of AZD4547 for 48 h. Cell viability was measured by MTT assay. The experiments were repeated thrice. Data were represented as mean ± SEM; $^{*}P < 0.05$; $^{**}P < 0.01$; $^{***}P < 0.001$

gration of BxPC-3 cells were impeded (Figs. 5E, 5F). Indeed, the expression of ERK signaling involved transcription factors were decreased in response to PD98059 as cordycepin did (Fig. 5G). Importantly, the cell cyclin-dependent kinase inhibitor p21 was activated and cyclin A2 was inhibited after the treatment of PD98059 (Fig. 5H). These results suggest that anti-tumor effects of cordycepin depend on FGFR-ERK signaling.

Cordycepin impeded tumor growth in vivo via interrupting FGFR / Ras / ERK signaling pathway

Based on the above results and the fact that cordycepin impeded the growth of BxPC-3 xenografts (Fig. 1E), we hypothesized that the downregulation of FGFR/Ras/ERK signaling by cordycepin may attribute to the inhibition of tumor

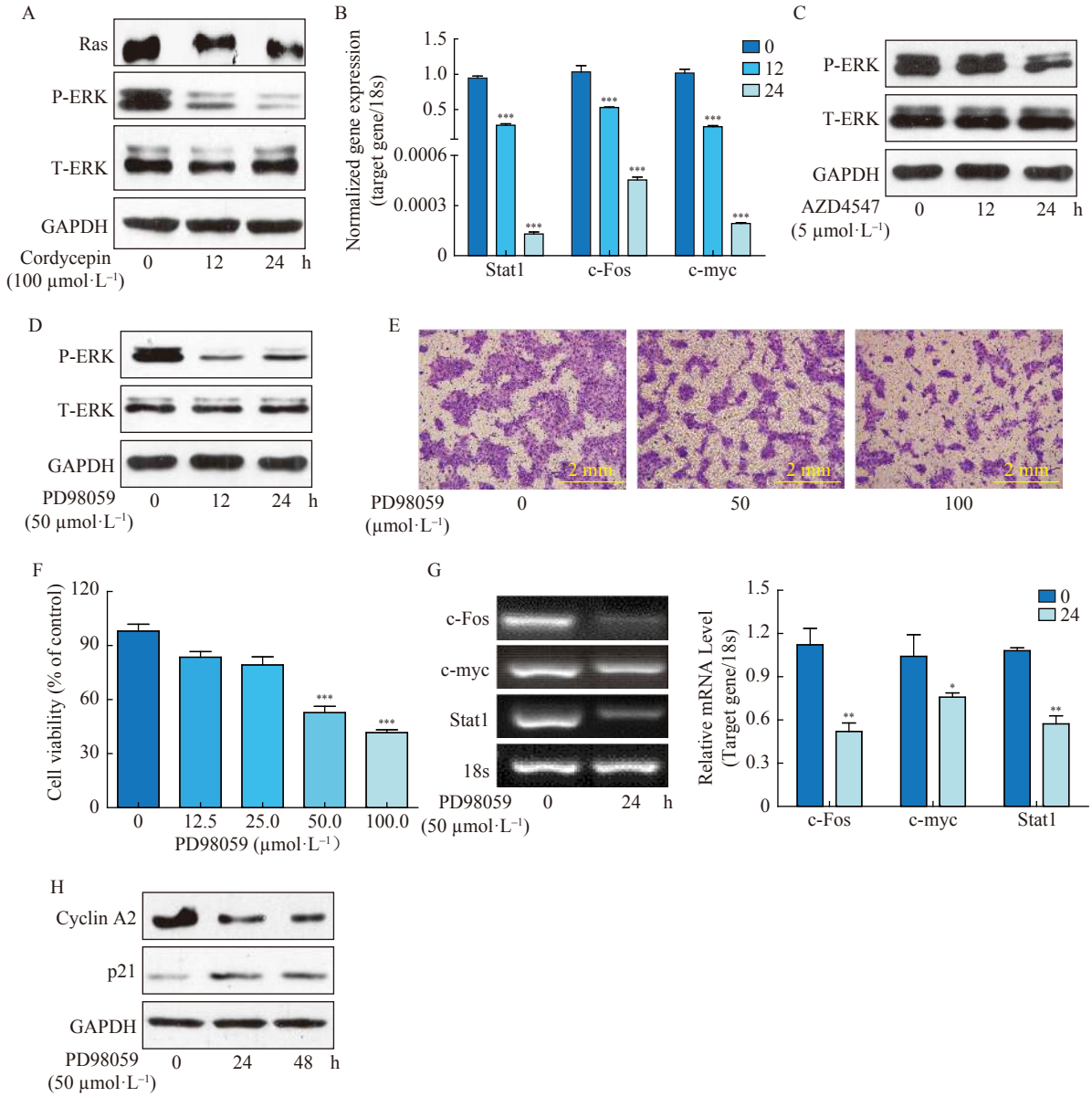

Fig. 5 Cordycepin caused cell death via inhibiting ERK pathway. (A) The expression of Ras and ERK phosphorylation were analyzed by Western blotting following treatment of BxPC-3 cells with 100 μmol·L^{-1} cordycepin for different time intervals. (B) After cordycepin treatment, the mRNA levels of stat1, c-Fos and c-myc were detected by Real-time PCR. (C) The expression of ERK phosphorylation was analyzed by Western blotting after 5 μmol·L^{-1} AZD4547 treatment for different time intervals. (D) Determination of ERK phosphorylation after PD98059 treatment by Western blotting. (E) The migration of BxPC-3 cells was examined by Transwell assay after PD98059 treatment for 8 h. (F) BxPC-3 cells were incubated with indicated concentrations of PD98059 for 48 h. Then cell viability was measured by MTT assay. (G) BxPC-3 cells were treated with 100 μmol·L^{-1} for indicated time. RT-PCR was used to analyze mRNA levels of c-Fos, c-myc and stat1. Integrated optical densities of bands normalized by 18s were shown in the right of the picture. (H) The expression of p21 and cyclin A2 was measured by Western blotting. The experiments were repeated thrice. Data were represented as mean ± SEM; $^{*}P < 0.05$; $^{**}P < 0.01$; $^{***}P < 0.001$

growth *in vivo*. In order to address this question, immunohistochemistry and Western blotting were employed to examine the related proteins in tumor tissue. The staining of cell proliferation marker Ki67 was lower in cordycepin treatment group compared to the control group (Fig. 6A). In addition, the phosphorylation of ERK in xenografted tumor tissues was downregulated after cordycepin treatment (Fig. 6B). Compared to the control group, the expression level of Ras and ERK phosphorylation was downregulated in cordycepin-treated xenografted tumors (Fig. 6C), which was consistent with *in vitro* results in response to cordycepin. These data suggested that cordycepin exerted anti-tumor effect *in vivo* might be through blocking FGFR/Ras/ERK signaling pathway.

Discussion

Pancreatic ductal adenocarcinoma is notorious for lack-

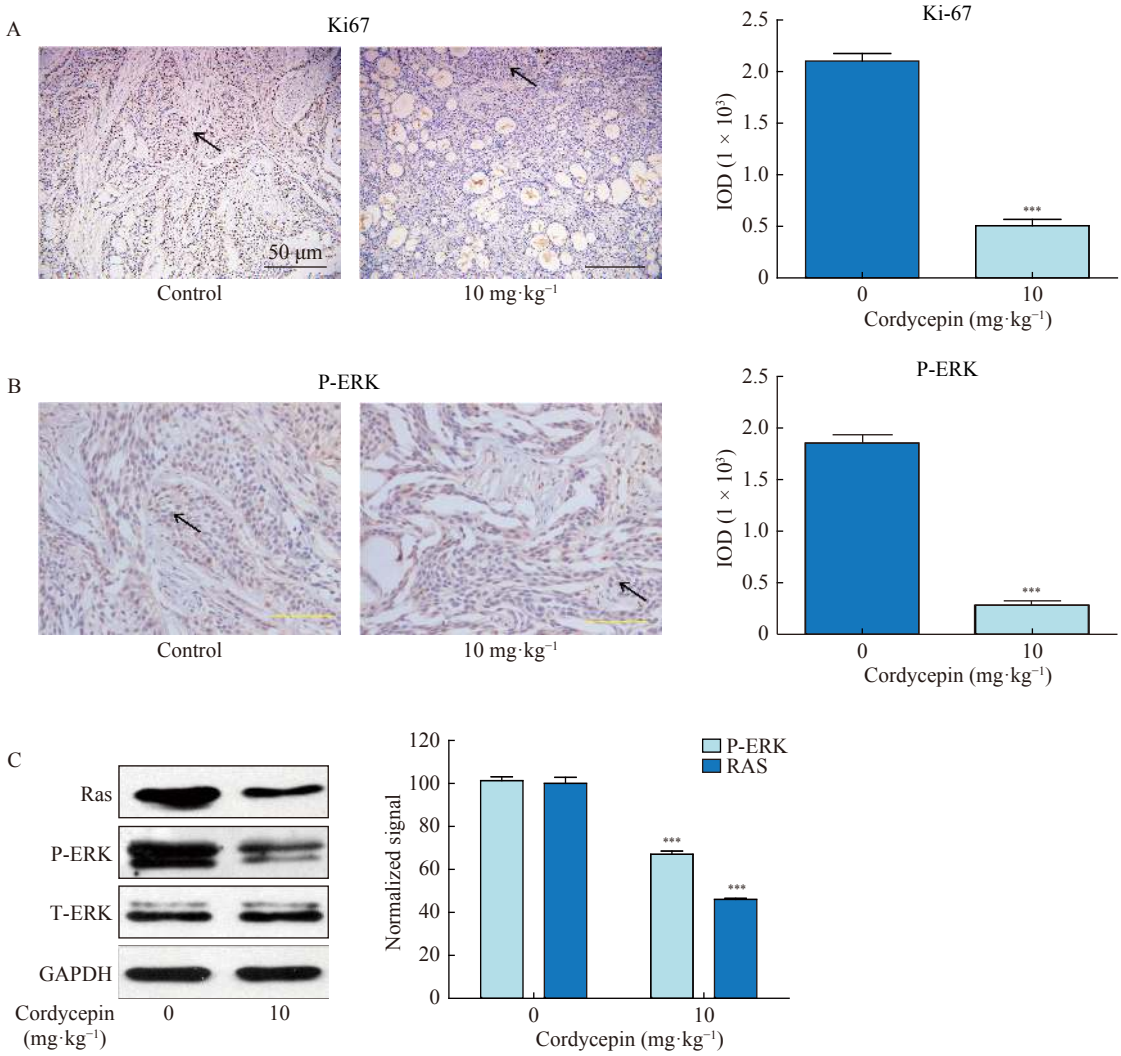

Fig. 6 Cordycepin impeded tumor growth *in vivo* via interrupting FGFR/Ras/ERK signaling pathway. Mice of experimental group were treated daily with 10 mg·kg^{-1} cordycepin via oral administration for 32 days, while the control animals were treated with equal volumes of normal saline. (A and B) The expressions of Ki67 (A) and ERK phosphorylation (B) were analyzed by immunohistochemistry (200 ×). The statistical analysis was shown on the right panels. (C) The expression of Ras and ERK phosphorylation in xenografted tumors were evaluated by Western blotting. Quantitative analysis of protein level was shown on the right panels. The experiments were repeated thrice. Data were represented as mean ± SEM; $^{***}P < 0.001$

ing of effective therapies [26]. In this study, we showed that cordycepin inhibited the migration of pancreatic cancer cell BxPC-3 *in vitro*. Also, cordycepin impeded BxPC-3 cells growth *in vitro* and *in vivo* by targeting FGFR2 and multiple signaling pathways.

We found that cordycepin treated-BxPC-3 cells released larger amount of cytochrome c from mitochondria to cytosol. Previous studies have shown that the release of cytochrome c could stimulate caspase-9 and caspase-3 and then trigger cell apoptosis [27-30], as we have seen in our study. The mRNA levels of FasL and Bax were upregulated after cordycepin treatment. It was reported that ERK Mitogen-activated protein kinase (MAPK) cascades were related to cell survival, proliferation, and differentiation [31]. In this study, ERK phosphorylation and Ras was inhibited by cordycepin in BxPC-3 cells. These results suggested that cordycepin triggered apoptosis via activating caspase signaling and affecting MAPK cascades in BxPC-3 cells.

Once DNA damage was triggered, ATM, ATR and Check point kinase2 (Chk2) were activated to regulated many cellular processes [32-35]. We demonstrated that phosphorylation of ATM, ATR and Chk2 was significantly upregulated by cordycepin (Fig. 3F). Afterwards, the activated Chk2 leaded to downregulation of CDK2 and Cyclin A2. Accordingly, these data suggested that cordycepin was ATM/ATR dependent to induce cell cycle arrest.

Aberrant FGFR signaling is a common phenotype in a variety of solid tumors and here is evidence that targeting FGFR could be therapeutically beneficial across PDAC [36]. In our study, cordycepin could strongly bind to FGFR2, the affinity of cordycepin to FGFR2 is similar to that of aFGF to FGFR2 (Figs. 4C, 4D). FGFRs activated various signaling

pathways, including ERK and PI-3 kinase signaling cascades [37, 38]. FGFR2 inactivation by cordycepin only led to disruption of ERK signaling pathway. Meanwhile, the ERK phosphorylation was also inhibited by FGFR2 inhibitor (AZD4547) in BxPC-3 cells (Fig. 5C). Furthermore, cell cycle was arrested by MEK inhibitor (PD98059) via activating p21 and inhibiting cyclin A2 (Fig. 5H). FGFR activation had been reported to recruit PI-3 kinase and then stimulate PI-3 kinase [39]. However, in our study, cordycepin treatment had no influence on PI-3 kinase signaling pathway (Fig. S1). The experimental results indicated that cordycepin targeted FGFR2 to impede Erk MAPK signaling pathway which was a novel regulatory mechanism inhibited BxPC-3 cells growth. Importantly, to our knowledge, *in vivo* model was firstly studied to evaluate anti-tumor efficacy of cordycepin on pancreatic cancer.

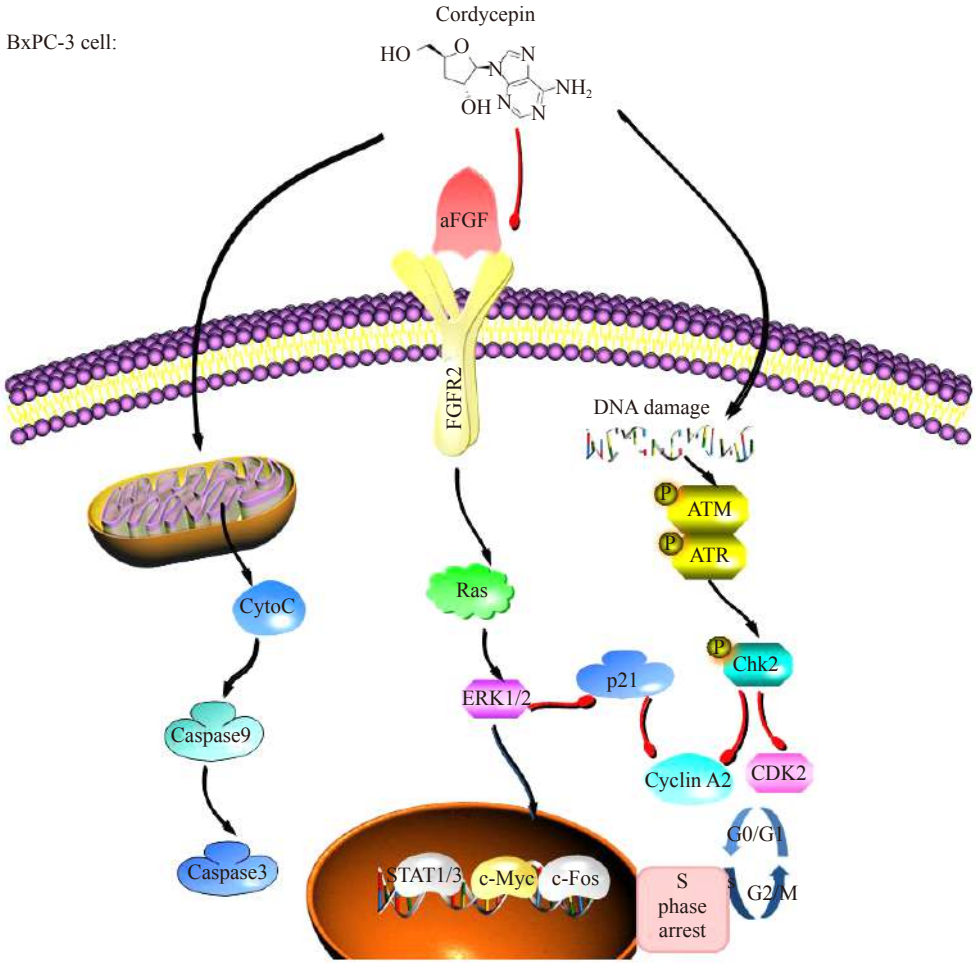

Fig. S1 Schematic representation of cordycepin-induced pancreatic cancer cells BxPC-3 apoptosis via caspase, Chk2 and FGFR/Ras/ERK signaling pathways. Cordycepin triggered cell apoptosis through activating cytochrome c, caspase-3 and caspase-9. Cordycepin could interact with FGFR2, the downstream ERK MAPK signaling and its transcription factors (C-Fos, c-myc and stat1) were inhibited. In response to cordycepin induce a cascade of events, including the activation of ATM, ATR, Chk2 and p21. Afterwards downregulating the P-CDK2 and Cyclin A2 results in the induction of cell cycle arrest. Meanwhile, the decrement of ERK phos-phorylation could activate p21 and lead to cell cycle arrest

Taken together, Cordycepin could be a potential candidate for the treatment of pancreatic ductal adenocarcinoma.

Conclusions

Taken together, cordycepin may target FGFR2 and impede Ras/ERK signaling pathway and further inhibit pancreatic cancer BxPC-3 cells growth *in vitro* and *in vivo*, and induce the cells apoptosis by activating caspase-3, caspase-9 and cytochrome c. The results suggest that cordycepin may potentially be a leading compound or a new drug candidate for the treatment of pancreatic ductal adenocarcinoma.

References

[1] Miller KD, Siegel RL, Lin CC, *et al*. Cancer treatment and survivorship statistics, 2016 [J]. *CA Cancer J Clin*, 2016, **66**(4): 271–289.

[2] Siegel RL, Miller KD, Jemal A. Cancer statistics, 2016 [J]. *CA Cancer J Clin*, 2016, **66**(1): 7–30.

[3] Bergman AM, Pinedo HM, Peters GJ. Determinants of resistance to 2',2'-difluorodeoxycytidine (gemcitabine) [J]. *Drug Resist Updat*, 2002, **5**(1): 19–33.

[4] de Sousa Cavalcante L, Monteiro G. Gemcitabine: metabolism and molecular mechanisms of action, sensitivity and chemoresistance in pancreatic cancer [J]. *Eur J Pharmacol*, 2014, **741**: 8–16.

[5] Itoh N, Ornitz DM. Evolution of the Fgf and Fgfr gene families [J]. *Trends Genet*, 2004, **20**(11): 563–569.
[6] Eswarakumar VP, Lax I, Schlessinger J. Cellular signaling by fibroblast growth factor receptors [J]. *Cytokine Growth Factor Rev*, 2005, **16**(2): 139–149.
[7] Baird A, Esch F, Mormede P, *et al*. Molecular characterization of fibroblast growth factor: distribution and biological activities in various tissues [J]. *Recent Prog Horm Res*, 1986, **42**: 143–205.
[8] Lieu C, Heymach J, Overman M, *et al*. Beyond VEGF: inhibition of the fibroblast growth factor pathway and antiangiogenesis [J]. *Clin Cancer Res*, 2011, **17**(19): 6130–6139.
[9] Greenman C, Stephens P, Smith R, *et al*. Patterns of somatic mutation in human cancer genomes [J]. *Nature*, 2007, **446**(7132): 153–158.
[10] Kuniyasu H, Abbruzzese JL, Cleary KR, *et al*. Induction of ductal and stromal hyperplasia by basic fibroblast growth factor produced by human pancreatic carcinoma [J]. *Int J Oncol*, 2001, **19**: 681–685.
[11] Kouhara H, Hadari YR, Spivak-Kroizman T, *et al*. A lipid-anchored Grb2-binding protein that links FGF-receptor activation to the Ras/MAPK signaling pathway [J]. *Cell*, 1997, **89**(5): 693–702.
[12] Roberts PJ, Der CJ. Targeting the Raf-MEK-ERK mitogen-activated protein kinase cascade for the treatment of cancer [J]. *Oncogene*, 2007, **26**(22): 3291–3310.
[13] McCubrey JA, Steelman LS, Chappell WH, *et al*. Roles of the Raf/MEK/ERK pathway in cell growth, malignant transformation and drug resistance [J]. *Biochim Biophys Acta*, 2007, **1773**(8): 1263–1284.
[14] Pan BS, Wang YK, Lai MS, *et al*. Cordycepin induced MA-10 mouse Leydig tumor cell apoptosis by regulating p38 MAPKs and PI3K/AKT signaling pathways [J]. *Sci Rep*, 2015, **5**: 13372.
[15] Tian X, Li Y, Shen Y, *et al*. Apoptosis and inhibition of proliferation of cancer cells induced by cordycepin [J]. *Oncol Lett*, 2015, **10**(2): 595–599.
[16] Wang Z, Wu X, Liang YN, *et al*. Cordycepin induces apoptosis and inhibits proliferation of human lung cancer cell line H1975 via inhibiting the phosphorylation of EGFR [J]. *Molecules*, 2016, **21**(10): 1267.
[17] Zhang Y, Zhang XX, Yuan RY, *et al*. Cordycepin induces apoptosis in human pancreatic cancer cells via the mitochondrial-mediated intrinsic pathway and suppresses tumor growth *in vivo* [J]. *Onco Targets Ther*, 2018, **11**: 4479–4490.
[18] Chang MM, Pan BS, Wang CY, *et al*. Cordycepin-induced unfolded protein response-dependent cell death, and AKT/MAPK-mediated drug resistance in mouse testicular tumor cells [J]. *Cancer Med*, 2019, **00**: 1–16.
[19] Hadari YR, Kouhara H, Lax I, *et al*. Binding of Shp2 tyrosine phosphatase to FRS2 is essential for fibroblast growth factor-induced PC12 cell differentiation [J]. *Mol Cell Biol*, 1998, **18**(7): 3966–3973.
[20] Zhang Z, Tudi T, Liu Y, *et al*. Preparative isolation of cordycepin, N(6)-(2-hydroxyethyl)-adenosine and adenosine from Cordyceps militaris by macroporous resin and purification by recycling high-speed counter-current chromatography [J]. *J Chromatogr B Analyt Technol Biomed Life Sci*, 2016, **1033–1034**: 218–225.
[21] Thornberry NA, Lazebnik Y. Caspases: enemies within [J]. *Science*, 1998, **281**(5381): 1312–1316.
[22] Li P, Nijhawan D, Budihardjo I, *et al*. Cytochrome c and dATP-dependent formation of Apaf-1/caspase-9 complex initiates an apoptotic protease cascade [J]. *Cell*, 1997, **91**(4): 479–489.
[23] Yang E, Zha J, Jockel J, *et al*. Bad, a heterodimeric partner for Bcl-XL and Bcl-2, displaces Bax and promotes cell death [J]. *Cell*, 1995, **80**(2): 285–291.
[24] Chibazakura T, Kamachi K, Ohara M, *et al*. Cyclin A promotes S-phase entry via interaction with the replication licensing factor Mcm7 [J]. *Mol Cell Biol*, 2011, **31**(2): 248–255.
[25] Harper JW, Adami GR, Wei N, *et al*. The p21 Cdk-interacting protein Cip1 is a potent inhibitor of G1 cyclin-dependent kinases [J]. *Cell*, 1993, **75**(4): 805–816.
[26] Wu ZS, Liu CF, Fu B, *et al*. Suramin blocks interaction between human FGF1 and FGFR2 D2 domain and reduces downstream signaling activity [J]. *Biochem Biophys Res Commun*, 2016, **477**(4): 861–867.
[27] Erkan M, Hausmann S, Michalski CW, *et al*. The role of stroma in pancreatic cancer: diagnostic and therapeutic implications [J]. *Nat Rev Gastroenterol Hepatol*, 2012, **9**(8): 454–467.
[28] Kroemer G, Dallaporta B, Resche-Rigon M. The mitochondrial death/life regulator in apoptosis and necrosis [J]. *Annu Rev Physiol*, 1998, **60**: 619–642.
[29] Yanase N, Ohshima K, Ikegami H, *et al*. Cytochrome c release, mitochondrial membrane depolarization, caspase-3 activation, and Bax-alpha cleavage during IFN-alpha-induced apoptosis in Daudi B lymphoma cells [J]. *J Interferon Cytokine Res*, 2000, **20**(12): 1121–1129.
[30] Chae HJ, Chae SW, An NH, *et al*. Cyclic-AMP inhibits nitric oxide-induced apoptosis in human osteoblast: the regulation of caspase-3,-6,-9 and the release of cytochrome c in nitric oxide-induced apoptosis by cAMP [J]. *Biol Pharm Bull*, 2001, **24**(5): 453–460.
[31] Chipuk JE, Bhat M, Hsing AY, *et al*. Bcl-xL blocks transforming growth factor-beta 1-induced apoptosis by inhibiting cytochrome c release and not by directly antagonizing Apaf-1-dependent caspase activation in prostate epithelial cells [J]. *J Biol Chem*, 2001, **276**(28): 26614–26621.
[32] Seger R, Krebs EG. The MAPK signaling cascade [J]. *FASEB J*, 1995, **9**(9): 726–735.
[33] Savitsky K, Bar-Shira A, Gilad S, *et al*. A single ataxia telangiectasia gene with a product similar to PI-3 kinase [J]. *Science*, 1995, **268**(5218): 1749–1753.
[34] Bensimon A, Schmidt A, Ziv Y, *et al*. ATM-dependent and -independent dynamics of the nuclear phosphoproteome after DNA damage [J]. *Sci Signal*, 2010, **3**(151): rs3.
[35] Pires IM, Olcina MM, Anbalagan S, *et al*. Targeting radiation-resistant hypoxic tumour cells through ATR inhibition [J]. *Br J Cancer*, 2012, **107**(2): 291–299.
[36] Matsuoka S, Huang M, Elledge SJ. Linkage of ATM to cell cycle regulation by the Chk2 protein kinase [J]. *Science*, 1998, **282**(5395): 1893–1897.
[37] Helsten T, Elkin S, Arthur E, *et al*. The FGFR landscape in cancer: analysis of 4853 tumors by next-generation sequencing [J]. *Clin Cancer Res*, 2016, **22**(1): 259–267.
[38] Lax I, Wong A, Lamothe B, *et al*. The docking protein FRS2alpha controls a MAP kinase-mediated negative feedback mechanism for signaling by FGF receptors [J]. *Mol Cell*, 2002, **10**(4): 709–719.
[39] Wong A, Lamothe B, Lee A, *et al*. FRS2 alpha attenuates FGF receptor signaling by Grb2-mediated recruitment of the ubiquitin ligase Cbl [J]. *Proc Natl Acad Sci U S A*, 2002, **99**(10): 6684–6689.

Cite this article as: LI Xue-Ying, TAO Hong, JIN Can, DU Zhen-Yun, LIAO Wen-Feng, TANG Qing-Jiu, DING Kan. Cordycepin inhibits pancreatic cancer cell growth *in vitro* and *in vivo* via targeting FGFR2 and blocking ERK signaling [J]. *Chin J Nat Med*, 2020, **18**(5): 345-355.